Episcopic three-dimensional (3D) imaging involves novel techniques that create volume data by capturing images of subsequent surfaces of blocks containing histologically processed and embedded specimens during their physical sectioning on microtomes. Such techniques have been used for creating 3D computer models in morphologic studies[10,11]. Of the techniques, episcopic fluorescence image capture (EFIC)[12,13] and high-resolution episcopic microscopy[14] have been successfully applied in recent research, while other applications, such as fast 3D serial reconstruction[15], surface imaging microscopy[16,17], and serial block-face scanning electron microscopy[18], are not yet routine and only preliminary results are currently available.

EFIC was designed for analyzing the morphology of the organ systems of normal and malformed embryos[12,13,19]. The specimens are embedded in a reddish-stained medium on a wax base. Then, monochrome light is applied to the block surface in order to excite autofluorescence of the tissues. EFIC has higher image resolution than other 3D imaging modalities, such as magnetic resonance microscopy[12,20–22], with fewer artifacts compared with conventional histologic methods. EFIC utilizes autofluorescent signal originating from pyridine nucleotides[12,20], which exist in every cell of the body. High-intensity regions imply high cell density or high proliferation rate. The structural components of the knee during the prenatal period have been visualized, but never using EFIC. For example, with EFIC, the joint cavities may be clearly recognizable as low-density areas because they contain few cells.

In the present study, taking advantage of EFIC, development of the knee joint was morphologically investigated, and the process of cavitation was analyzed using spatial and temporal 3D reconstructions.

Materials and methods

Animals

Fifty hindlimbs (25 right, 25 left) were removed from 25 white Wister rat embryos between E14 and E20, except for E15 (E14, $n = 3$; E16, $n = 2$; E17, 18, 19, 20, $n = 5$ each). Wister rats were obtained from SHIMIZU Laboratory Supplies Co., Ltd (Kyoto, Japan). All of the mother rats were sacrificed by pentobarbital sodium overdose before caesarean section. Whole rat embryos were fixed immediately after removal from the uterus in 4% paraformaldehyde at 4°C overnight before dissecting the hindlimbs. Samples of the knee joint then were dehydrated in graded ethanol and xylene, according to conventional histologic processes.

Preparation and workflow for EFIC

Preparation of the samples for EFIC was performed as described elsewhere[12,13,19–21], with some modifications. Briefly, for EFIC, the dehydrated samples were infiltrated and embedded in 70.4% paraffin wax, containing 24.9% Vyber, 4.4% stearic acid, and 0.4% Sudan IV[21]. Incorporation of Sudan IV in the paraffin wax blocks fluorescence bleed-through from deeper layers of the tissue[20,21]. The paraffin blocks were sectioned using a Leica SM2500 sliding microtome (Leica Microsystems, Bannockburn, UK) at 5–7 μm. Autofluorescence at the paraffin block face was visualized using epifluorescence imaging with mercury illumination and a discosoma Redfilter (excitation/emission of 545/620 nm, respectively). Fluorescent images were captured using a Hamamatsu ORCA-ER low-light CCD camera (HAMAMATSU Photonics K.K., Shizuoka, Japan). The resolution of the camera was 300 pixels/inch, and pixel size was 1344 × 1024 pixels. The field of view ranged between 2352 × 1792 μm and 5672 × 4321 μm. Digital images of the tissues on the surfaces of the blocks containing the specimens were captured with the camera sitting on a magnifying optic[10,12,13,19–21]. The optical pathway of the optic was aligned precisely perpendicular to the block surface. After capturing an image of the block face, a small slice of the block was removed using the microtome blade. This slice permitted preservation of histologic sections for hematoxylin and eosin (H&E) staining. Then, a digital image of the freshly cut block surface was captured and the next slice of embedding block was removed. This procedure was repeated until the region of interest was sectioned and a stack of aligned digital images showing subsequent block faces with tissues of the specimens was produced. Optical magnification ranged between ×25 and ×60, whereas the digital resolution ranged between 1.75 and 4.22 μm^2/pixel.

Analysis

Two-dimensional (2D) image stacks obtained by EFIC were reconstructed using OsiriX 4.0 (Pixmeo SARL, Geneva, Switzerland). These 2D images were resectioned digitally to generate sagittal, transverse, and coronal sections. The parts of interest of the knee, such as cavity, ligament, and meniscus, were segmented on 2D serial sections manually and then reconstructed three-dimensionally without smoothing using AMIRA 5.4.0 software (Visage, Berlin, Germany). Manual segmentation of each lesion was performed by three individual researchers (RT, ZX, and HS), according to the criteria for that anatomic portion, and assessed by two individual observers (TA and TT). The results of segmentation were almost equal. Volume of the joint cavity was calculated as an integration of the area on 2D serial images using the same software.

Ethics

All of the experiments with animals were approved by the Institutional Animal Research Committee and performed according to the Guidelines for Animal Experiments of Kyoto University.

Statistical analysis

All data are shown as mean ± SD. The software program SPSS Statistics (IBM, Armonk, NY) was used for statistical analysis. Differences in volume between the FPC and the other five cavities (described in the Results section) at each developmental stage was assessed using the Student's t test. Significant differences between the FPC and the other cavities at the same time interval were expressed using a length of the 95% confidence interval (CI). One-way analysis of variance (ANOVA) and the Tukey–Kramer test were performed to examine differences in cavity volume among developmental stages.

Results

Comparison of EFIC and H&E staining

Major components of the knee joint were distinguishable as different signal intensities on EFIC after the E17 stage (Fig. 1). The periosteum [Fig. 1(A)] and ligaments [Fig. 1(A), asterisk] showed relatively high autofluorescent intensity due to dense distribution of the cells, whereas, cartilaginous anlagen showed lower autofluorescent intensity [Fig. 1(A)]. Each component of the knee joint was clearly distinguishable by its intensity according to the proceeding of development. The cavity had low intensity [Fig. 1(B), arrow], while the border of the cavity had high intensity [Fig. 1(B), arrowhead]. In particular, just before cavity formation [Fig. 1(C) [ii], arrowhead], the signal intensity of the border increased [Fig. 1(C) [i], arrow].

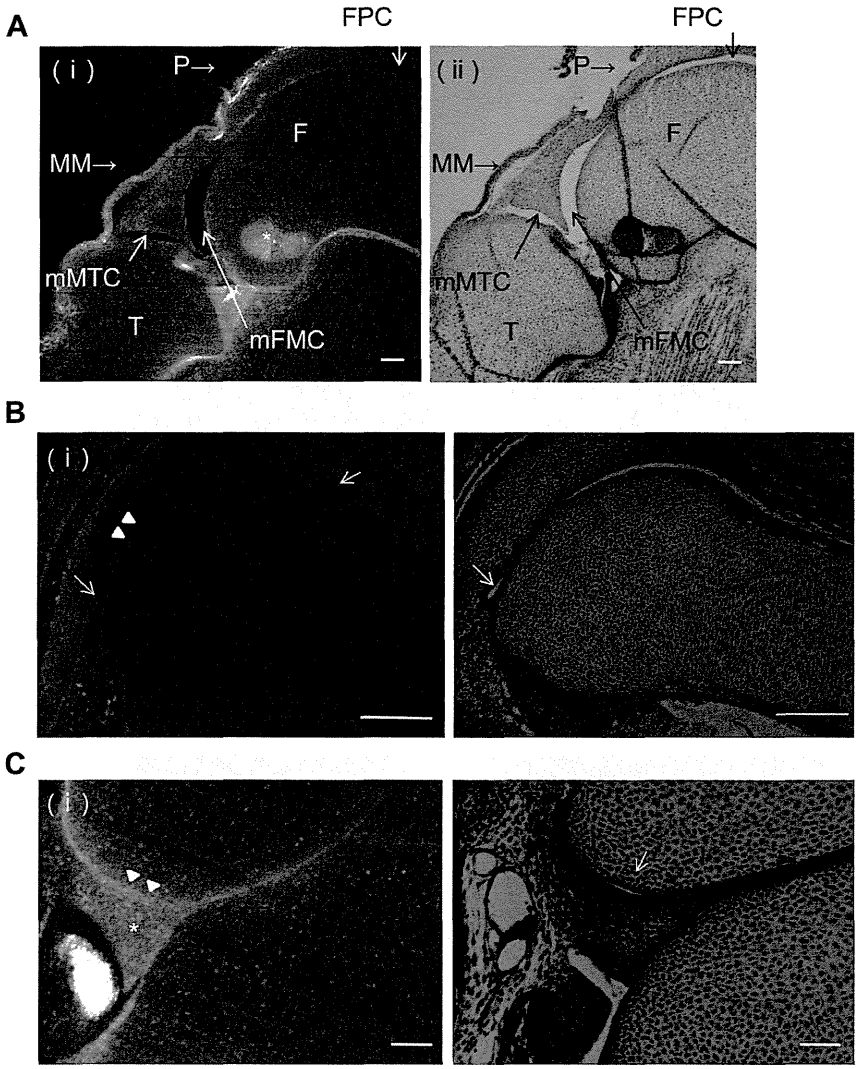

Fig. 1. EFIC and corresponding histologic section with hematoxylin and eosin staining. A: Representative sagittal section of the knee joint at embryonic day (E) 20, captured using EFIC (i), and corresponding histologic section with hematoxylin and eosin (H&E) staining (ii). Major components of the knee joint were recognizable on both EFIC image and histologic section. The cross section of the PCL is shown as an area of high intensity (*). Magnification ×50. Resolution = 2.11 μm^2/pixel. Bar = 100 μm. Abbreviations: F, femur; P, patella; T, tibia. B: Sagittal section of the knee joint at E17, captured using EFIC (i), and corresponding histologic section with H&E staining (ii). The arrow represents the cavity, while the arrowhead represents the border of the cavity. Magnification ×100. Resolution = 1.06 μm^2/pixel. Bar = 100 μm. C: Sagittal section of the knee joint at E20, captured using EFIC (i), and corresponding histologic section with H&E staining (ii). The arrow represents the cavity, while the arrowhead represents the border of cavity. The anlage of the meniscus is shown as an area of high intensity (*). Magnification ×200. Resolution = 1.06 μm^2/pixel. Bar = 100 μm.

Morphogenesis of the knee joint

Development of the knee joint cavity from E16 to E20 was precisely observed using EFIC and then analyzed with 3D reconstructions.

The structures of bone anlagen and interzone were not observed in the presumptive areas of limb bone formation in all three specimens at E14 (data not shown).

A low-intensity area corresponding to chondrification was observed in the femur, tibia, and fibula in the two specimens at E16 [Fig. 2(A)]. A three-layered structure corresponding to interzone also was seen between the femur and tibia in the two specimens at E16 [Fig. 2(B)]. First, we observed a couple of samples at each embryonic stage. However, the joint cavity was not observed before E16. Therefore, the sample number was added ($n = 5$) and quantification of the joint cavity was performed in the samples after E17.

The joint cavities were named based on position and place according to Gray's description[7]: FPC, mFMC, lFMC, mMTC, lMTC, and circumligament cavity (CLC). Analogs of the anterior cruciate ligament (ACL) and posterior cruciate ligament (PCL) were initially recognizable as faint lines with high intensity at E17 [Fig. 3(A) [ii]]. The lateral meniscus (LM) [Fig. 3(A) [i]] and medial meniscus (MM) [Fig. 3(A) [iii]] were recognizable as a high-intensity triangular shape connecting to the surface mesenchymal tissues at the joint. The patella was observed as a low-intensity area, whereas, the patellar ligament was seen as a relatively high-intensity area [Fig. 1(B) [i], Fig. 3(A) [ii]]. The initial joint cavity formed simultaneously at the FPC, mFMC, and lFMC in four out of five specimens [Fig. 3(A), (B)]. The FPC had a notch-like formation from both the cranial and caudal sides of the patella [Fig. 1(B) [i], Fig. 3(A) [ii]]. The mFMC was observed as a large distinct cavity, while the lFMC was seen as several small dots. No cavities were observed around the ACL or PCL in the five specimens.

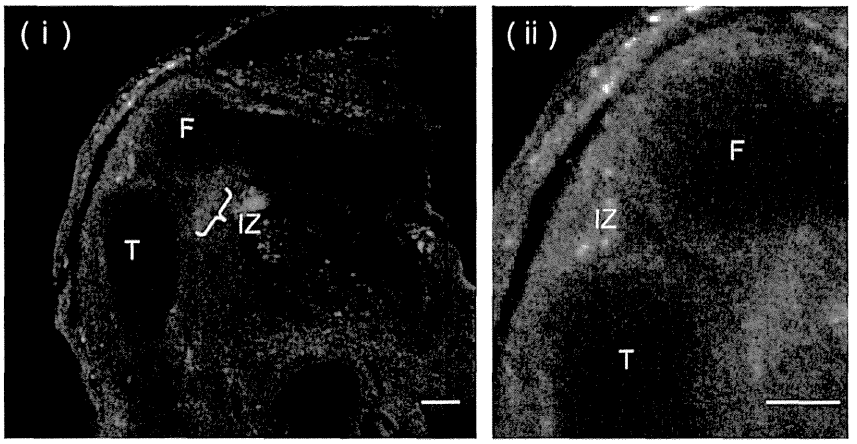

Fig. 2. EFIC at embryonic day (E) 16. Representative sagittal section of the right knee joint at E16 (i), and higher magnification (ii). Chondrification of the femur (F), tibia (T), and fibula (not shown) can be observed. A three-layered structure can be seen between the femur and tibia, indicating the interzone (IZ). Magnification ×25. Resolution = 4.22 μm^2/pixel. Bar = 100 μm.

Initiation of cavitation at the mMTC and lMTC was detected for the first time in three out of five specimens at E18 [Fig. 4(A) [iii]]. The FPC and mFMC became large distinct cavities, but the lFMC was still small. A lining of high intensity around the cavity also was detected. At this stage, small cavities around the ACL and PCL were detected in four out of five specimens. This cavity could not be classified into the traditional five classifications (i.e., FPC, mFMC, lFMC, mMTC, and lMTC), so we named it the CLC.

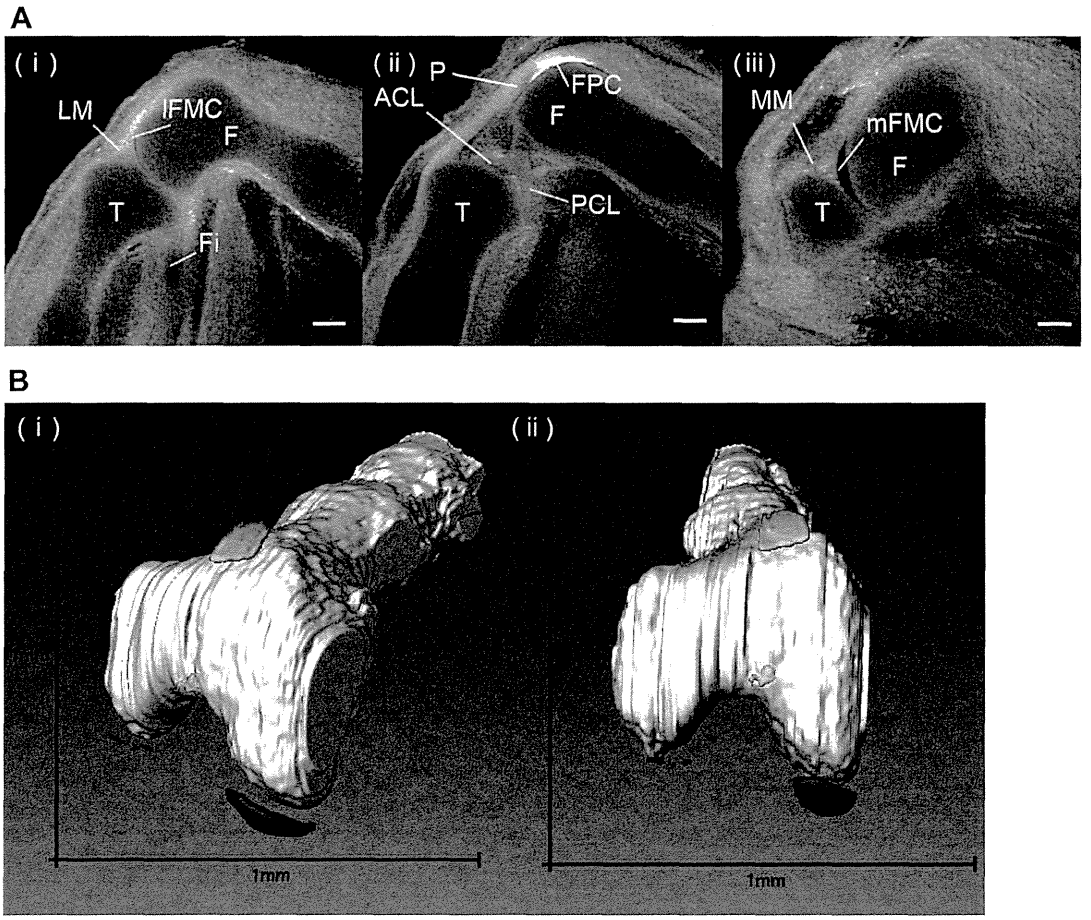

Fig. 3. EFIC at embryonic day (E) 17. A: Representative lateral (i), intermediate (ii), and medial (iii) sagittal sections of the right knee joint at E17. Magnification ×60. Resolution = 1.75 μm^2/pixel. Bar = 100 μm. Abbreviations: F, femur; Fi, fibula; P, patella; T, tibia. B: Three-dimensional reconstruction of the right knee joint at E17.White, femur; green, FPC; purple, lateral and medial femoromeniscal cavities.

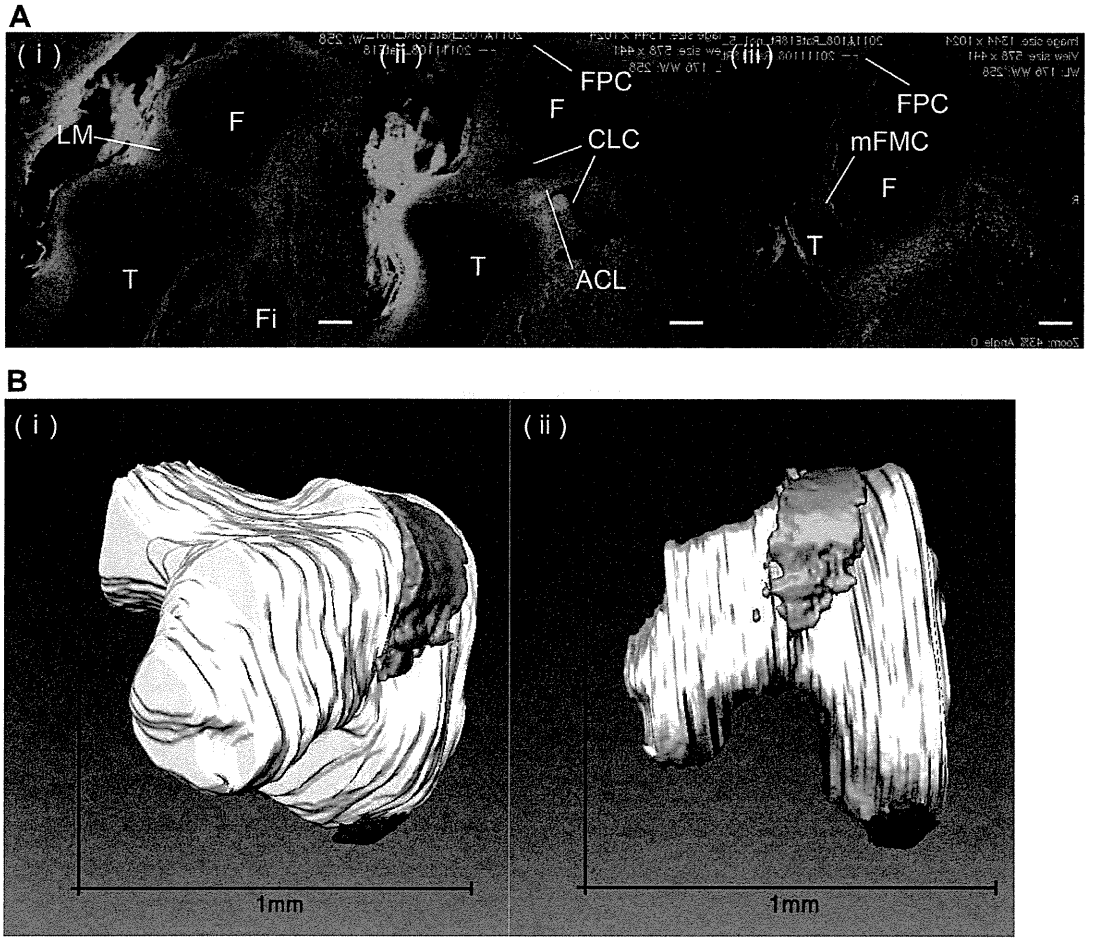

Fig. 4. EFIC at embryonic day (E) 18. A: Representative lateral (i), intermediate (ii), and medial (iii) sagittal sections of the right knee joint at E18. Magnification ×50. Resolution = 2.11 μm²/pixel. Bar = 100 μm. Abbreviations: F, femur; Fi, fibula; T, tibia. B: Three-dimensional reconstruction of the right knee joint at E18.White, femur; green, FPC; purple, lateral and medial femoromeniscal and circumligament cavities.

Each component of the knee joint—femur, tibia, fibula, ligaments, and menisci—were well defined at E19 [Fig. 5]. The patella also was clearly differentiated, the ACL and PCL became sharp and thick, and the FPC became a large space. The mMTC and lMTC became large and connected with the mFMC and lFMC, respectively, in three out of five specimens. The cavities of the medial side were always larger than those of the lateral side. At this stage, the knee cavity was separated into three parts since the cavities around the ACL and PCL were limited.

Autofluorescent intensity at both cruciate ligaments and the lining around the cavity increased, showing a contrast to other tissues, at E20 [Fig. 6(A)]. Although the cruciate ligaments were initially observed as an area of high intensity at E17 (Fig. 3), they were clearly recognizable as mature constructs at E20 [Fig. 6(A) [ii]]. Cavitations around the ACL and PCL proceeded, connecting all cavities together.

Morphometry of cavity formation

The volume of the FPC and the other five cavities (mFMC, lFMC, mMTC, lMTC, and CMC) at each developmental stage was measured (Fig. 7). The volume of the FPC increased significantly between E17 and E20 ($P = 0.002$), E18 and E20 ($P = 0.003$), and E19 and E20 ($P = 0.009$). The volume of the other five cavities also increased significantly between E17 and E20 ($P = 0.007$), E18 and E20 ($P = 0.009$), and E19 and E20 ($P = 0.047$). The volume of the FPC preceded that of the other cavities, but not to a significant degree (E17: 95% CI, −1.043 to 1.480; E18: 95% CI, −1.859 to 4.447; E19: 95% CI, −0.064 to 8.367; E20: 95% CI, −24.660 to 36.789).

Discussion

In the present study, the spatial and temporal process of knee joint cavity formation was described using EFIC and 3D reconstructions. The primary findings were as follows: Cavitation began from six portions, including the cranial and caudal sides of the FPC, mFMC, and lFMC, at E17. Cavitation of the MTC followed at E18. Cavitations of the medial side of the MTC preceded those of the lateral side. All cavities were connected at E20 when cavitations around the ACL and PCL were completed.

The EFIC system had several advantages in the present analysis. Joint cavities are mechanically fragile and prone to interference by artifacts during histologic preparation. In this regard, EFIC has a great advantage in that much fewer artifacts are expected compared with conventional histologic methods[10,12,13,19–22]. The firm embedded block was imaged and no staining was required in EFIC, whereas, thin sectioned samples were observed after staining in the conventional histologic method. In addition, joint cavities were clearly recognizable as very low-density areas in EFIC, as expected. High-intensity regions on EFIC images imply high cell

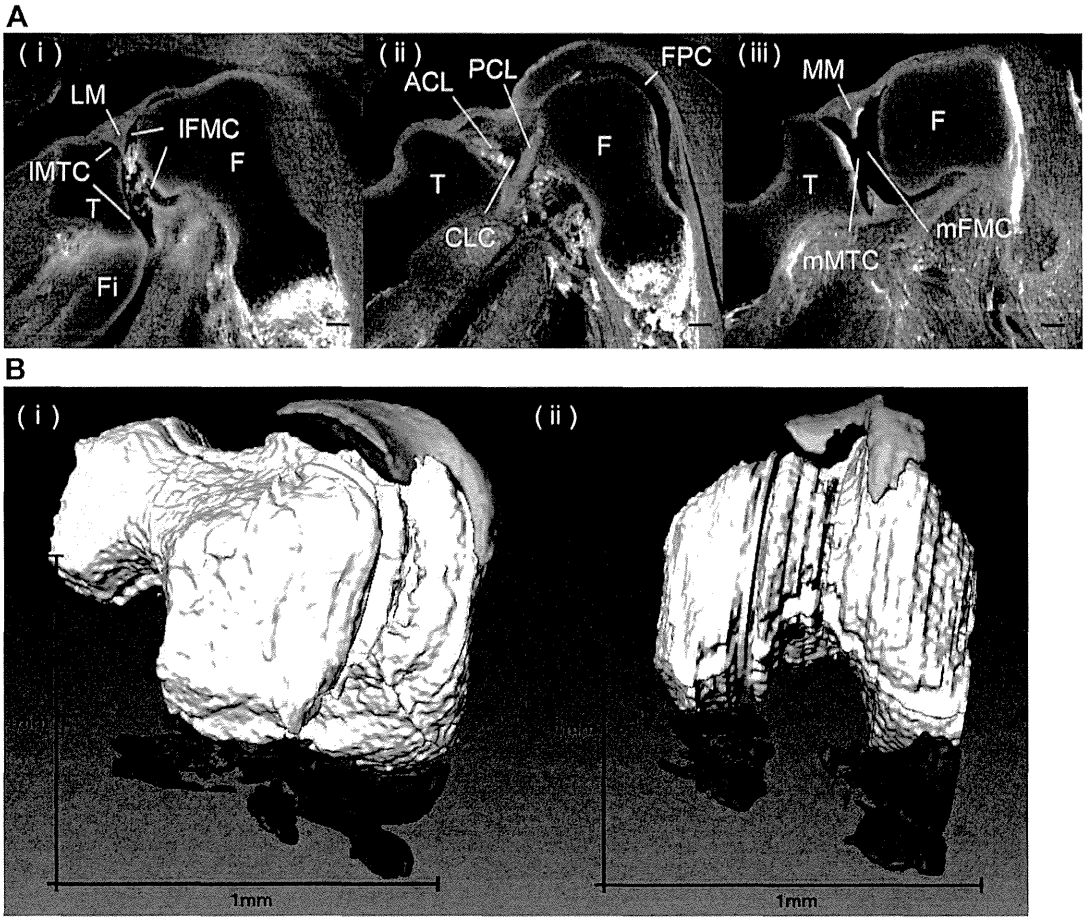

Fig. 5. EFIC at embryonic day (E) 19. A: Representative lateral (i), intermediate (ii), and medial (iii) sagittal sections of the right knee joint at E19. Magnification ×45. Resolution = 2.34 μm²/pixel. Bar = 100 μm. Abbreviations: F, femur; Fi, fibula; T, tibia. B: Three-dimensional reconstruction of the right knee joint at E19White, femur; green, FPC; purple, lateral and medial femoromeniscal, lateral and medial meniscotibial, and circumligament cavities.

density or high proliferative rate[12,20]. In this point of view, it should be noted that the border of the cavity was highlighted as a linear structure with high intensity, indicating the presence of well-proliferating cell groups [Fig. 1(B), (C)]. In histologic analysis, a single-layered cell was recognizable after E17 [Fig. 1(B) [ii], arrowhead]. The process of cavitation seems to be affected by multiple factors, including mechanical forces generated from muscle contraction[23], increase of hyaluronan and hyaluronan-binding protein synthesis[24,25], and decrease of collagen fibrils in the interzone[8]. Ito and Kida reported that the mechanism of joint cavitation was based on proliferation and immigration of cells in the intermediate zone rather than apoptotic cell death[8]. Whether or not the cells at the high-intensity line are involved in the process of cavitation is subject to further study.

EFIC data may suggest the existence of a novel proliferative area, which had not been properly recognized before. Each component of the joint had changing signal intensity during development. The triangular area, which became the meniscus at later stages, was recognizable as an area of high intensity [Fig. 1(C) [i], asterisk]. A high-intensity area was detected at the peripheral area of the triangle facing the joint cavity [Fig. 1(C) [i], arrowhead], demonstrating the initiation of joint cavity formation. This area later connected to the high-intensity lining at the border of the cavity. The migration of cells from the intermediate zone to around the cavity has been shown in a previous study[8]. The migrated cells may accumulate and increase the density of the cells, especially in the peripheral area of the triangle. The cruciate ligaments were another component in which the signal intensity gradually increased until E20. Usually, the cell density of the ligaments is low in adults. The kinetics of the cells in the ligaments during development is variable and worth studying.

The formation of suprapatellar and popliteal cysts is a clinically pathogenic condition[26]. Crnković mentioned that the suprapatellar cyst developed in the embryonic stage as a separate synovial lesion[26]. The suprapatellar cyst perforates and communicates with the patellofemoral compartment in the fifth month of fetal life[26]. Although we could not observe a clear septum between the suprapatellar cyst and the FPC, the finding of active cavity formation may support the results of the report and lead to better understanding of formation of suprapatellar and popliteal cysts.

In the current study, formation of the medial condyle and mFPC preceded that of the lateral portion. In humans, development of the medial condyle precedes that of the lateral condyle[27], but it remains unknown whether or not the mFPC precedes the lFPC. In adult humans, the structure of the knee joint is asymmetric[27,28]. This asymmetry is clinically important as it influences the mechanism, capability, and also disease of the knee joint; even bilateral variation of the knee joint is the lowest in the human body[29]. For example, asymmetry of the trochlear groove influences patellar tracking. The patella starts from a slight lateral tilt and then tilts

Fig. 6. EFIC at embryonic day (E) 20. A: Representative lateral (i), intermediate (ii), and medial (iii) sagittal sections of the right knee joint at E20. Magnification ×50. Resolution = 2.11 μm^2/pixel. Bar = 100 μm. Abbreviations: F, femur; Fi, fibula; P, patella; T, tibia. B: Three-dimensional reconstruction of the right knee joint at E20. The patella is not fully reconstructed and is seen only partially. White, femur; green, FPC; purple, lateral and medial femoromeniscal, lateral and medial meniscotibial, and circumligament cavities; orange, patella; light blue, ACL; blue, PCL.

medially until 40°of flexion, laterally until 100°of flexion, then sharply medially beyond 100° of flexion[30]. This abnormal tracking induces osteoarthritis of the patellofemoral joint. Although the structure of the knee joint is different between mice and humans, surgical traumatic osteoarthritis models in mice have been recognized as useful for human osteoarthritis models[30–34].

In summary, the spatial and temporal process of knee joint cavity formation in rat embryos between E14 and E20 was

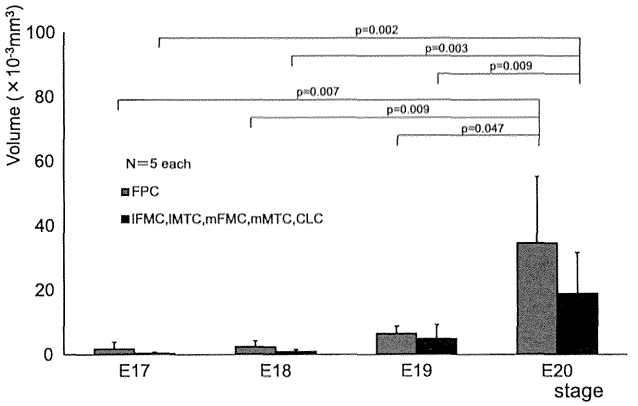

Fig. 7. Morphometry of cavity formation in each developmental stage. Volume of the FPC (green) and the other five cavities (purple, mFMC, lFMC, mMTC, lMTC, and CLC) at each developmental stage was measured. Values are mean ± 95% confidence interval.

described with 3D reconstructions. Cavitation began from five separate portions at E17, and proceeded asymmetrically. All cavities were connected at E20 when cavitations around the ACL and PCL were completed. The EFIC system had advantages in the present 3D analysis. These results will contribute to a better understanding of the structural feature and pathology of the knee joint.

Conclusion

Cavity formation initiated from six portions. In each portion, development proceeded asymmetrically. These results concerning anatomic development of the knee joint using EFIC will contribute to a better understanding of the structural feature of the knee joint.

Author contributions

Ryota Takaishi performed the experiments, interpreted the data, and drafted the manuscript. Tomoki Aoyama provided financial support, designed the study, and drafted the manuscript. Xiangkai Zhang performed the experiments and interpreted the data. Shinya Higuchi performed the experiments and interpreted the data. Shigehito Yamada provided financial support and technical guidance. Tetsuya Takakuwa provided financial support and final approval of the manuscript to be submitted.

Role of the funding source

This study was supported by grants #22591199, #24119002, #25461642, and #23300199 from the Japan Society for the Promotion of Science and BIRD of the Japan Science and Technology Agency.

Conflict of interest statement

There are no conflicts of interest.

Acknowledgments

The authors thank Rune Fujioka, Akira Ito, Junichi Tajino, Momoko Nagai, Shoki Yamaguchi, Hirotaka Iijima, and Hiroshi Kuroki for their skilled technical assistance and advice.

References

1. Kenney RR. The synovial joints: a review of the literature. J Am Osteopath Assoc 1966;65(10):1092–7.
2. Berumen-Nafarrate E, Leal-Berumen I, Luevano E, Solis FJ, Muñoz-Esteves E. Synovial tissue and synovial fluid. J Knee Surg 2002;15(1):46–8.
3. Goldring MB, Tsuchimochi K, Ijiri K. The control of chondrogenesis. J Cell Biochem 2006;97(1):33–44.
4. Dowthwaite GP, Edwards JC, Pitsillides AA. An essential role for the interaction between hyaluronan and hyaluronan binding proteins during joint development. J Histochem Cytochem 1998;46(5):641–51.
5. Wagner M. Functional anatomy of the knee joint (In German). Orthopade 1987;16(2):88–99.
6. Ralphs JR, Benjamin M. The joint capsule: structure, composition, ageing and disease. J Anat 1994;184(Pt 3):503–9.
7. Gray DJ, Gardner E. Prenatal development of the human knee and superior tibiofibular joints. Am J Anat 1950;86(2):235–87.
8. Ito MM, Kida MY. Morphological and biochemical re-evaluation of the process of cavitation in the rat knee joint: cellular and cell strata alterations in the interzone. J Anat 2000;197(Pt 4):659–79.
9. Gardner E, O'Rahilly R. The early development of the knee joint in staged human embryos. J Anat 1968;102(Pt 2):289–99.
10. Weninger WJ, Geyer SH. Episcopic 3D imaging methods: tools for researching gene function. Curr Genomics 2008;9(4):282–9.
11. Weninger WJ, Meng S, Streicher J, Müller GB. A new episcopic method for rapid 3-D reconstruction: applications in anatomy and embryology. Anat Embryol 1998;197(5):341–8.
12. Weninger WJ, Mohun T. Phenotyping transgenic embryos: a rapid 3-D screening method based on episcopic fluorescence image capturing. Nat Genet 2002;30(1):59–65.
13. Mohun TJ, Weninger WJ. Episcopic three-dimensional imaging of embryos. Cold Spring Harb Protoc 2012;2012(6):641–6.
14. Weninger WJ, Geyer SH, Mohun TJ, Rasskin-Gutman D, Matsui T, Ribeiro I, *et al.* High-resolution episcopic microscopy: a rapid technique for high detailed 3D analysis of gene activity in the context of tissue architecture and morphology. Anat Embryol 2006;211(3):213–21.
15. Odgaard A, Andersen K, Melsen F, Gundersen HJ. A direct method for fast three-dimensional serial reconstruction. J Microsc 1990;159(Pt 3):335–42.
16. Ewald AJ, McBride H, Reddington M, Fraser SE, Kerschmann R. Surface imaging microscopy, an automated method for visualizing whole embryo samples in three dimensions at high resolution. Dev Dyn 2002;225:369–75.
17. Gerneke DA, Sands GB, Ganesalingam R, Joshi P, Caldwell BJ, Smaill BH, *et al.* Surface imaging microscopy using an ultramiller for large volume 3D reconstruction of wax- and resin-embedded tissues. Microsc Res Tech 2007;70(10):886–94.
18. Denk W, Horstmann H. Serial block-face scanning electron microscopy to reconstruct three-dimensional tissue nanostructure. PLoS Biol 2004;2(11):e329.
19. Weninger WJ, Floro KL, Bennett MB, Withington SL, Preis JI, Barbera JP, *et al.* Cited2 is required both for heart morphogenesis and establishment of the left-right axis in mouse development. Development 2005;132(6):1337–48.
20. Rosenthal J, Mangal V, Walker D, Bennett M, Mohun TJ, Lo CW. Rapid high resolution three dimensional reconstruction of embryos with episcopic fluorescence image capture. Birth Defects Res C Embryo Today 2004;72(3):213–23.
21. Yamada S, Samtani RR, Lee ES, Lockett E, Uwabe C, Shiota K, *et al.* Developmental atlas of the early first trimester human embryo. Dev Dyn 2010;239(6):1585–95.
22. Tsuchiya M, Yamada S. High-resolution histological 3D-imaging: episcopic fluorescence image capture (EFIC) is widely applied for experimental animals. Congenit Anom (Kyoto) 2014, http://dx.doi.org/10.1111/cga.12057.

23. Roddy KA, Prendergast PJ, Murphy P. Mechanical influences on morphogenesis of the knee joint revealed through morphological, molecular and computational analysis of immobilised embryos. PLoS One 2011;6(2):e17526.
24. Dowthwaite GP, Ward AC, Flannely J, Suswillo RF, Flannery CR, Archer CW, *et al.* The effect of mechanical strain on hyaluronan metabolism in embryonic fibrocartilage cells. Matrix Biol 1999;18(6):523–32.
25. Dowthwaite GP, Flannery CR, Flannelly J, Lewthwaite JC, Archer CW, Pitsillides AA. A mechanism underlying the movement requirement for synovial joint cavitation. Matrix Biol 2003;22(4):311–22.
26. Crnković T, Gašpar D, Ethurović D, Podsednik D, Slišurić F. New insights about suprapatellar cyst. Orthop Rev (Pavia) 2012; 4(1):e9.
27. Varich LJ, Laor T, Jaramillo D. Normal maturation of the distal femoral epiphyseal cartilage: age-related changes at MR imaging. Radiology 2000;214(3):705–9.
28. Bindelglass DF, Dorr LD. Current concepts review: symmetry versus asymmetry in the design of total knee femoral components—an unresolved controversy. J Arthroplasty 1998;13(8):939–44.
29. Plochocki JH. Bilateral variation in limb articular surface dimensions. Am J Hum Biol 2004;16(3):328–33.
30. Rhoads DD, Noble PC, Reuben JD, Mahoney OM, Tullos HS. The effect of femoral component position on patellar tracking after total knee arthroplasty. Clin Orthop Relat Res 1990;260: 43–51.
31. Mollenhauer JA, Erdmann S. Introduction: molecular and biomechanical basis of osteoarthritis. Cell Mol Life Sci 2002; 59(1):3–4.
32. Brandt KD. Animal models of osteoarthritis. Biorheology 2002;39(1–2):221–35.
33. Glasson SS, Blauchet TJ, Morris EA. The surgical destabilization of the medical meniscus (DMM) model of osteoarthritis in the 129/SvEv mouse. Osteoarthritis Cartilage 2007;15(9):1061–9.
34. Chia WT, Pan RY, Tseng FJ, Chen YW, Feng CK, Lee HS, *et al.* Experimental osteoarthritis induced by surgical realignment of the patella in BALB/c mice. J Bone Joint Surg Br 2010;92(12): 1710–6.

Geriatrics Gerontology INTERNATIONAL Medline Indexed

Geriatr Gerontol Int 2014; **14:** *758–762*

ORIGINAL ARTICLE: EPIDEMIOLOGY, CLINICAL PRACTICE AND HEALTH

Effect of physical activity on memory function in older adults with mild Alzheimer's disease and mild cognitive impairment

Takanori Tanigawa,[1] Hajime Takechi,[2] Hidenori Arai,[1] Minoru Yamada,[1] Shu Nishiguchi[1] and Tomoki Aoyama[1]

[1]Department of Physical Therapy, Human Health Sciences, and [2]Department of Geriatric Medicine, Graduate School of Medicine, Kyoto University, Kyoto, Japan

Aim: It is very important to maintain cognitive function in patients with mild cognitive disorder. The aim of the present study was to determine whether the amount of physical activity is associated with memory function in older adults with mild cognitive disorder.

Methods: A total of 47 older adults with mild cognitive disorder were studied; 30 were diagnosed with mild Alzheimer's disease and 17 with mild cognitive impairment. The global cognitive function, memory function, physical performance and amount of physical activity were measured in these patients. We divided these patients according to their walking speed (<1 m/s or >1 m/s). A total of 26 elderly patients were classified as the slow walking group, whereas 21 were classified as the normal walking group.

Results: The normal walking group was younger and had significantly better scores than the slow walking group in physical performance. Stepwise multiple linear regression analysis showed that only the daily step counts were associated with the Scenery Picture Memory Test in patients of the slow walking group ($\beta = 0.471$, $P = 0.031$), but not other variables. No variable was significantly associated with the Scenery Picture Memory Test in the normal walking group.

Conclusions: Memory function was strongly associated with the amount of physical activity in patients with mild cognitive disorder who showed slow walking speed. The results show that lower physical activities could be a risk factor for cognitive decline, and that cognitive function in the elderly whose motor function and cognitive function are declining can be improved by increasing the amount of physical activity. **Geriatr Gerontol Int 2014; 14: 758–762.**

Keywords: memory function, mild cognitive disorder, older adults, physical activity, physical performance.

Introduction

Mild cognitive impairment (MCI) is a condition of objective cognitive impairment based on neuropsychological testing in the absence of clinically overt dementia.[1] This condition is of interest for identifying the prodromal and transitional stages of Alzheimer's disease (AD)[2,3] and other types of dementia. Indeed, a study shows that more than half of MCI cases progress to dementia within 5 years.[1] However, it is reported that the cognitive function of people with MCI can recover to normal.[4,5] Indeed, one study showed that 38.5% of older adults with MCI recovered to normal within 5 years.[6] Therefore, it is very important to prevent the deterioration of MCI to dementia. Because no consensus has been established regarding pharmacological intervention for MCI, non-pharmacological intervention is expected. Accordingly, we need to establish a way to prevent deterioration or even improve cognitive function in MCI patients.

Recently, it has attracted attention that increasing the amount of physical activity can prevent the decline of cognitive function. Many studies reported that global cognitive function is associated with the amount of physical activity. Furthermore, previous reports have shown that physical frailty is associated with an increased risk of developing AD and MCI,[8,9] and can predict a future cognitive decline in older adults.[10] Additionally, people with dementia have been shown to be

Accepted for publication 20 August 2013.

Correspondence: Dr Tomoki Aoyama MD PhD, Department of Physical Therapy, Human Health Sciences, Graduate School of Medicine, Kyoto University, 53 Kawahara-cho, Shogoin, Sakyo-ku, Kyoto 606-8507, Japan. Email: aoyama.tomoki.4e@kyoto-u.ac.jp

frail because of their poor mobility and body composition.[11,12] Thus, cognitive function and physical frailty are interrelated.

Accordingly, the cognitive decline in frail elderly patients can cause further decline of cognitive function and motor function. Therefore, it is important to maintain and improve the cognitive function of the frail elderly with mild cognitive disorder.

Several studies have shown the relationship between cognitive decline that can be observed at the early stage of dementia and the amount of physical activity. However, no study has addressed whether the association between cognitive function and the amount of physical activity depends on the level of motor function in MCI or mild AD patients.

Therefore, the aim of the present study was to determine whether there is an association between memory function and the amount of physical activity in older adults with mild cognitive disorder, stratified by their motor function.

Methods

Participants

We recruited patients from the memory clinic of the Department of Geriatric Medicine in Kyoto University Hospital, Kyoto, Japan. The diagnosis of AD or MCI was made according to the following criteria: AD, *Diagnostic and Statistical Manual of Mental Disorders*, 4th edition, and the National Institute of Neurological and Communicative Disorders and Stroke and the Alzheimer's Disease and Related Disorders Association;[13,14] and MCI, Petersen's criteria.[15] Of the 47 patients with cognitive disorder, 30 were classified as mild AD and 17 as MCI by the criteria. In the present study, we did not set the upper and lower limits of the Mini-Mental State Examination (MMSE) for the diagnosis of MCI. The exclusion criteria used in the present study were vascular dementia, dementia with Lewy bodies, lacunar infarcts, Fazekas grade 3 periventricular hyperintensity/deep white-matter hyperintensity,[16] severe cardiac, pulmonary or musculoskeletal disorders, or the presence of comorbidities associated with an increased risk of falls, such as Parkinson's disease and stroke.

Written informed consent for the trial was obtained from each participant or his/her family members in accordance with the guidelines approved by the Kyoto University Graduate School of Medicine and the Declaration of Human Rights, Helsinki, 1975.

Walking speed

Comfortable 10-m walking time (walking time) is a simple test developed to screen basic mobility performance in frail older adults. It has been reported that the elderly with a walking score greater than 10.0 s can suffer an increased risk of falling.

Therefore, we divided the participants into two groups according to their walking speed (cut-off: 1 m/s); 26 of the older adults were classified as the normal walking group, whereas 21 of the older adults were classified as the slow walking group.

Cognitive function measures

Cognitive function was assessed by the MMSE and the Scenery Picture Memory Test (SPMT). MMSE is a global cognitive test that can be used to systematically and thoroughly assess mental status. It is an 11-question measure that tests five areas of cognitive function: orientation, registration, attention and calculation, recall, and language. The maximum score is 30. A score of 23 or lower is indicative of cognitive impairment. SPMT is a short and simple memory test assessing the visual memory encoded as scenery, combined with verbal answers. Briefly, it uses a line drawing scenery picture of a living room in a house where 23 objects commonly observed in daily life are drawn on an A4 piece of paper. The examinee is instructed to look at the picture for 1 min and remember the items. After this encoding period, we distracted participants by asking them to carry out a brief digits forward test. Participants were then asked to recall the objects in the picture without time limitation. This recall time usually takes less than 1 min. The number of items recalled is the score for SPMT. Higher scores indicate better cognitive function. We have previously shown that SPMT is a quick and effective screen for MCI.[17]

Physical performance measures

The participants were asked to carry out the three motor function tests that are widely used to identify the frail elderly. For each performance task, the participants carried out two trials, and the better performance of the two was used for the analysis. Physical performance assessments, such as walking time,[18] the Timed Up & Go (TUG) test,[19] the Functional Reach test,[20] the one-leg stand (OLS) test,[21] and the five chair stand test (5CS)[22] were carried out as previously described.

Physical activity measures

In physical activity, a valid, accurate and reliable pedometer, the Yamax Power walker EX-510, was used to measure the free-living step counts.[23] The participants were instructed to wear the pedometer in their pocket on the side of their dominant leg for 14 consecutive days except when bathing, sleeping or carrying out water-based activities. This pedometer has a 30-day data storage capacity. We calculated the averages of their daily step counts for 2 weeks.

Table 1 Comparison of demographic characteristics and measurements with the overall group, normal walking group, and slow walking group

	All (= 47)	Normal walking (= 26)	Slow walking (= 21)	*P*-value
Age (years)	76.9 ± 7.0	74.7 ± 7.2	79.6 ± 5.9	0.016*
Female sex, *n* (%)	28 (59.6%)	17 (65.4%)	11 (52.4%)	0.38
BMI	21.7 ± 3.7	22.1 ± 3.7	21.1 ± 3.8	0.36
Loneliness	5 (10.6%)	2 (7.7%)	3 (14.3%)	0.64
Donepezil treatment	41 (87.2%)	24 (92.3%)	17 (81.0%)	0.39
MMSE	23.4 ± 3.6	23.0 ± 3.1	24.0 ± 4.2	0.37
SPMT	6.5 ± 4.7	6.7 ± 5.1	6.1 ± 4.4	0.68
Physical activity	4371.9 ± 3605.9	5264.0 ± 3476.9	3267.4 ± 3532.5	0.06
10 m walking time	9.9 ± 2.3	8.2 ± 1.0	12.3 ± 1.6	<0.001***
TUG time	9.5 ± 2.7	7.9 ± 1.4	11.4 ± 2.6	<0.001***
OLS	11.9 ± 15.8	16.9 ± 19.3	5.8 ± 6.1	0.01*
5CS	11.1 ± 3.5	10.0 ± 2.2	12.4 ± 4.2	0.016*

5CS, five chair stand test; BMI, body mass index; MMSE, Mini-Mental State examination; OLS, one leg standing; SPMT, Scenery Picture Memory Test; TUG, Timed Up & Go test. *$P < 0.05$ ***$P < 0.001$.

Statistical analysis

The *t*-test and χ^2-test were used to compare the data between the normal and slow walking groups. Multiple linear regression analysis using a stepwise method was carried out to investigate whether physical activity, age, sex, body mass index, TUG, OLS and 5CS were independently associated with SPMT. The data were analyzed using SPSS software Windows version 20.0 (SPSS, Chicago, IL, USA). A *P*-value <0.05 was considered statistically significant for all analyses.

Results

The demographic characteristics of the overall, normal and slow walking groups are summarized in Table 1. A total of 26 patients were classified as the normal walking group, and 21 patients as the slow walking group. There were no significant differences in sex, body mass index, loneliness, donepezil treatment, SPMT or physical activity between the two groups ($P > 0.05$). The normal walking group was younger (normal walking group 74.7 ± 7.2, slow walking group 79.6 ± 5.9, $P = 0.016$), and had significantly better scores than the slow walking group in TUG (normal walking group 7.9 ± 1.4 s, slow walking group 11.4 ± 2.6 s, $P < 0.001$), OLS (normal walking group 24.3 ± 24.3 s, slow walking group 5.8 ± 6.1 s, $P = 0.006$), 5CS (normal walking group 10.0 ± 2.2 s, slow walking group 12.4 ± 4.2 s, $P = 0.016$; Table 1). In the slow walking group, physical activity was significantly correlated with SPMT ($r = 0.471$, $P = 0.031$), as shown in Figure 1, but this correlation was absent in the normal walking group. In addition, there was a correlation between SPMT and physical activity after adjusted by age and sex in the slow walking group ($r = 0.493$, $P = 0.032$).

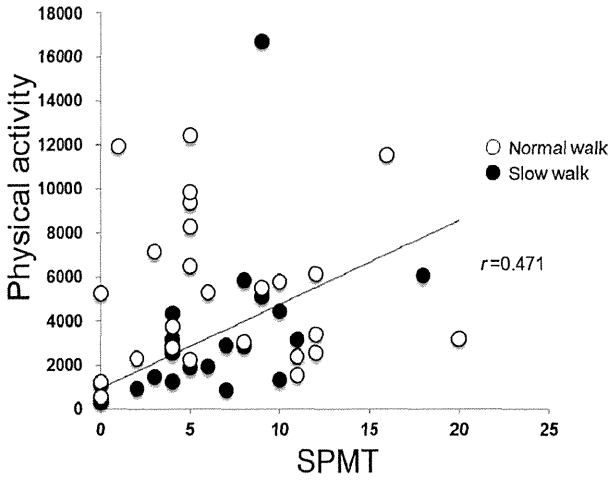

Figure 1 Relationship between physical activity and the Scenery Picture Memory Test (SPMT) in the normal walking and slow walking groups. In the slow walking group, physical activity was correlated significantly with SPMT ($r = 0.471$, $P = 0.031$).

Stepwise multiple linear regression analysis showed that no item was significantly associated with SPMT in the normal walking group, whereas only physical activity ($\beta = 0.471$, $P = 0.031$) was significantly associated with SPMT in the slow walking group (Table 2).

Discussion

The present study showed that memory function is strongly associated with the amount of physical activity

Table 2 Stepwise multiple regression analysis for Scenery Picture Memory Test

	Normal walking		Slow walking	
	β estimates	*P*-value	β estimates	*P*-value
Daily step counts	–	–	0.471	0.031*
Age	–	–	–	–
Sex	–	–	–	–
BMI	–	–	–	–
TUG time	–	–	–	–
OLS	–	–	–	–
5CS	–	–	–	–

Note: 5CS, five chair stand test; BMI, body mass index; OLS, one leg standing; TUG, Timed Up & Go test. *$P < 0.05$.

only in the slow walking group with mild cognitive disorder. The present results show that lower physical activity could be a risk factor for cognitive decline in the elderly, and would strengthen the evidence to show the relationship between the amount of physical activity and cognitive function, as previously reported.[24] Additionally, the present study might show that the cognitive function of the elderly whose motor function and cognitive function are declining can be improved by increasing the amount of physical activity.

Physical activity might have an impact on cognitive function. The reasons why the SPMT, not MMSE, showed a correlation with physical activity might be explained as following. First, SPMT has been developed to screen mild cognitive disorder, whereas the MMSE is usually used for a broad range of cognitive impairment from normal to severe dementia. Because we only included patients with mild cognitive disorder, SPMT might be better to detect small correlated changes with other functions than MMSE. Second, SPMT shows good correlation not only with memory tests, but also with frontal function tests including word fluency test (Takechi *et al.* unpubl. observation). We speculate that efficient reminding of many objects from the scene requires the frontal function. Third, SPMT uses a line drawing scenery picture of a living room familiar to the elderly. It has been reported that aerobic exercise induces beneficial changes in brain structure and function that are correlated with improvements in cognition,[25,26] even in AD patients.[27,28] Physical activity, such as walking in and out of doors, might concomitantly give the patients visual stimulation. Because SPMT uses a picture of a living room familiar to the elderly, the degree of visual stimulation in daily living might have affected the results of SPMT. Thus, physical activity and the capacity to remember a visual scene might have shown a correlation. We suggest that increasing the amount of physical activity might result in beneficial biological changes to the brain structure and function or in beneficial physical changes to mobility and body composition. Therefore, increasing the step counts in a day could help to maintain and improve the cognitive function of older adults with mild cognitive disorder.

In the normal walking group with mild cognitive disorder, we found no significant association between memory function and the other variables. Other studies also show a lack of association of cognitive function with the amount of physical activity in older adults with similar ages to those in the present study.[7,29] Therefore, we need to consider effective strategies for patients with higher physical function.

There were several limitations of the present study. First, our limited sample size might introduce some error of inference, reduce the power of the analysis and limit generalization. Second, the present study was a cross-sectional study. Therefore, the relationship between the memory function and physical activity needs further investigation, such as an increase in physical activity levels for a certain period can improve the scores of SPMT, MMSE and other cognitive tests. Third, the definition of the normal walking group depended only on walking time in the present study. We might have to measure a frailty index, such as the Edmonton frail scale[30] or the Fried frailty assessment,[31] if we can extend our results to the frail elderly. Fourth, we used the SPMT, a visual memory test, as a cognitive test. However, we did not measure other factors, such as visual function and attention, that might have affected the present results. Therefore, it might be impossible to evaluate properly the relationship between physical activity and memory function. Thus, the results of the present study should be interpreted with caution.

In conclusion, the present study shows that cognition is associated with higher levels of physical activity only in patients with mild cognitive disorder who showed a slow walking speed. Our results suggest that increasing the amount of physical activity might prevent the deterioration of cognitive function. Further investigation, such as a prospective study, is required to confirm our results.

Acknowledgments

This work was supported by Grants-in-Aid for Scientific Research from the Japan Society for the Promotion of Science, from the Ministry of Education, Culture, Sports, Science, and Technology.

Disclosure statement

None of the authors have conflicts of interest or financial disclosures.

References

1 McGough EL, Kelly VE, Logsdon RG *et al.* Associations between physical performance and executive function in older adults with mild cognitive impairment: gait speed and the Timed "Up & Go" test. *Phys Ther* 2011; **91**: 1198–1207.
2 Petersen RC, Doody R, Kurz A *et al.* Current concepts in mild cognitive impairment. *Arch Neurol* 2001; **58**: 1985–1992.
3 Winblad B, Palmer K, Kivipelto M *et al.* Mild cognitive impairment – beyond controversies, towards a consensus: report of the International Working Group on Mild Cognitive Impairment. *J Intern Med* 2004; **256**: 240–246.
4 Larrieu S, Letenneur L, Orgogozo JM *et al.* Incidence and outcome to mild cognitive impairment in a population-based prospective cohort. *Neurology* 2002; **59**: 1594–1599.
5 Matthews FE, Stephane BC, McLeith IG, Bond J, Brayne C. Two-year progression from mild cognitive impairment to dementia: to what extent do different definitions agree? *J Am Geriatr Soc* 2008; **56**: 1424–1433.
6 Ishikawa T, Ikeda M, Matsumoto N, Shigenobu K, Brayne C, Tanabe H. A longitudinal study regarding conversion from mild memory impairment to dementia in a Japanese community. *Int J Geriatr Psychiatry* 2006; **21**: 134–139.
7 Winchester J, Dick MB, Gillen D *et al.* Walking stabilizes cognitive functioning in Alzheimer's disease (AD) across one year. *Arch Gerontol Geriatr* 2013; **56** (1): 96–103.
8 Boyle PA, Buchman AS, Wilson RS, Leurgans SE, Bennett DA. Physical frailty is associated with incident mild cognitive impairment in community-based older persons. *J Am Geriatr Soc* 2010; **58**: 248–255.
9 Deshpande N, Metter EJ, Bandinelli S, Guralnik J, Ferrucci L. Gait speed under varied challenges and cognitive decline in older persons: a prospective study. *Age Ageing* 2009; **38**: 509–514.
10 Auyeung TW, Lee JS, Kwok T, Woo J. Physical frailty predicts future cognitive decline – a four-year prospective study in 2737 cognitively normal older adults. *J Nutr Health Aging* 2011; **15**: 690–694.
11 Cronin-Stubbs D, Beckett LA, Scherr PA *et al.* Weight loss in people with Alzheimer's disease: a prospective population based analysis. *BMJ* 1997; **314**: 178–179.
12 Scarmeas N, Albert M, Brandt J *et al.* Motor signs predict poor outcomes in Alzheimer's disease. *Neurology* 2005; **64**: 1696–1703.
13 American Psychiatric Association. *Diagnostic and Statistical Manual of Mental Disorders*, 4th edn. Washington, DC: American Psychiatric Association, 1994.
14 McKhann G, Drachman D, Folstein M, Katzman R, Price D, Stadlan EM. Clinical diagnosis of Alzheimer's disease: report of the NINCDS-ADRDA Work Group under the auspices of Department of Health and Human Services Task Force on Alzheimer's Disease. *Neurology* 1984; **34**: 939–944.
15 Petersen RC, Smith GE, Waring SC, Ivnik RJ, Tangalos EG, Kokmen E. Mild cognitive impairment: clinical characterization and outcome. *Arch Neurol* 1999; **56**: 303–308.
16 Fazekas F, Chawluk JB, Alavi A, Hurtig HI, Zimmerman RA. MR signal abnormalities at 1.5 T in Alzheimer's dementia and normal aging. *Am J Roentgenol* 1987; **149**: 351–356.
17 Takechi H, Dodge HH. Scenery Picture Memory Test: a new type of quick and effective screening test to detect early stage Alzheimer's disease patients. *Geriatr Gerontol Int* 2010; **10**: 183–190.
18 Lopopolo RB, Greco M, Sullivan D, Craik RL, Mangione KK. Effect of therapeutic exercise on gait speed in community-dwelling elderly people: a meta-analysis. *Phys Ther* 2006; **86**: 520–540.
19 Podsiadlo D, Richardson S. The timed "Up & Go": a test of basic functional mobility for frail elderly persons. *J Am Geriatr Soc* 1991; **39**: 142–148.
20 Duncan PW, Weiner DK, Chandler J, Studenski S. Functional reach: a new clinical measure of balance. *J Gerontol* 1990; **45**: M192–M197.
21 Vellas BJ, Wayne SJ, Romero L, Baumgartner RN, Rubenstein LZ, Garry PJ. One-leg balance is an important predictor of injurious falls in older persons. *J Am Geriatr Soc* 1997; **45**: 735–738.
22 Guralnik JM, Simonsick EM, Ferrucci L *et al.* A short physical performance battery assessing lower extremity function: association with self-reported disability and prediction of mortality and nursing home admission. *J Gerontol* 1994; **49**: M85–M94.
23 Crouter SE, Schneider PL, Karabulut M, Bassett DR Jr. Validity of 10 electronic pedometers for measuring steps, distance, and energy cost. *Med Sci Sports Exerc* 2003; **35**: 1455–1460.
24 Abbott RD, White LR, Ross GW, Masaki KH, Curb JD, Petrovitch H. Walking and dementia in physically capable elderly men. *JAMA* 2004; **292**: 1447–1453.
25 Cotman CW, Berchtold NC. Exercise: a behavioral intervention to enhance brain healthy and plasticity. *Trends Neurosci* 2002; **25**: 295–301.
26 Nichol KE, Parachikova AI, Cotman CW. Three weeks of running wheel exposure improves cognitive performance in the aged Tg2576 mouse. *Behav Brain Res* 2007; **184**: 124–132.
27 Yu F, Kolanowski AM. Facilitating aerobic exercise training in older adults with Alzheimer's disease. *Geriatric Nursing* 2009; **30**: 250–259.
28 Yu F, Kolanowski AM, Strumpf NE, Eslinger PJ. Improving cognition and function through exercise intervention in Alzheimer's disease. *J Nurs Scholarsh* 2006; **38**: 358–365.
29 Petersen RC. Mild cognitive impairment as a diagnostic entity. *J Intern Med* 2004; **56**: 183–194.
30 Rolfson DB, Majumdar SR, Tsuyuki RT, Tahir A, Rockwood K. Validity and reliability of the Edmonton Frail Scale. *Age Ageing* 2006; **35**: 526–529.
31 Fried LP, Tangen CM, Walston J *et al.* Frailty in older adults: evidence for a phenotype. *J Gerontol A Biol Sci Med Sci* 2001; **56A**: M146–M156.

TISSUE ENGINEERING: Part B
Volume 00, Number 00, 2014

DOI: 10.1089/ten.teb.2014.0090

An Exploratory Clinical Trial for Idiopathic Osteonecrosis of Femoral Head by Cultured Autologous Multipotent Mesenchymal Stromal Cells Augmented with Vascularized Bone Grafts

Tomoki Aoyama, MD, PhD,[1–3] Koji Goto, MD, PhD,[2,*] Ryosuke Kakinoki, MD, PhD,[2,4] Ryosuke Ikeguchi, MD, PhD,[2,†] Michiko Ueda, BA,[3] Yasunari Kasai, BSc,[5] Taira Maekawa, MD, PhD,[5,6] Harue Tada, PhD,[7] Satoshi Teramukai, PhD,[7,‡] Takashi Nakamura, MD, PhD,[2,§] and Junya Toguchida, MD, PhD[2,3,8]

Idiopathic osteonecrosis of femoral head (ION) is a painful disorder that progresses to collapse of the femoral head and destruction of the hip joint. Although its precise pathology remains unknown, the loss of blood supply causing the loss of living bone-forming cells is a hallmark of the pathophysiology of osteonecrosis. Transplantation of multipotent mesenchymal stromal cells (MSCs) is a promising tool for regenerating the musculoskeletal system. The aim of the present study was to assess the safety and efficacy of transplantation of cultured autologous bone marrow-derived MSCs mixed with β-tricalcium phosphate (β-TCP) in combination with vascularized bone grafts for the treatment of advanced stage ION in a clinical trial. Ten patients with stage 3 ION were enrolled in this study. Autologous bone marrow-derived MSCs were cultured with autologous serum, and cells ($0.5–1.0 \times 10^8$) were transplanted after mixing with β-TCP granules in combination with vascularized iliac bone grafts. Patients were assessed 24 months after treatment. The primary and secondary endpoints were progression of the radiological stage and changes in bone volume at the femoral head, and clinical score, respectively. Nine of ten patients completed the protocol, seven of whom remained at stage 3, and the remaining two cases progressed to stage 4. The average bone volume increased from $56.5 \pm 8.5\,cm^3$ to $57.7 \pm 10.6\,cm^3$. The average clinical score according to the Japan Orthopaedic Association improved from 65.6 ± 25.5 points to 87.9 ± 19.0 points. One severe adverse event was observed, which was not related to the clinical trial. Although the efficacy of cell transplantation was still to be determined, all procedures were successfully performed and some young patients with extensive necrotic lesions with pain demonstrated good bone regeneration with amelioration of symptoms. Further improvements in our method using MSCs and the proper selection of patients will open a new approach for the treatment of this refractory disease.

Introduction

IDIOPATHIC OSTEONECROSIS of femoral head (ION) is a painful disorder that progresses to collapse of the femoral head and symptomatic osteoarthritis of the hip joint.[1,2] This disease mainly affects individuals aged 30–40 years of age.[3] ION includes steroid-induced, alcoholism-related, and true idiopathic conditions. The precise pathological mechanism of ION remains unknown, however, macro- or microscopic obstruction of blood supply to the femoral head is considered to be a hallmark of this condition, which causes the necrosis of bone-forming cells. Bone tissues without bone-forming

[1]Department of Physical Therapy, Human Health Sciences, Graduate School of Medicine, Kyoto University, Kyoto, Japan.
[2]Department of Orthopaedic Surgery, Graduate School of Medicine, Kyoto University, Kyoto, Japan.
[3]Department of Tissue Regeneration, Institute for Frontier Medical Sciences, Kyoto University, Kyoto, Japan.
[4]Department of Rehabilitation Medicine, [5]Center for Cell and Molecular Therapy, and [6]Department of Transfusion Medicine and Cell Therapy, Kyoto University Hospital, Kyoto, Japan.
[7]Department of Clinical Trial Design and Management, Translational Research Center, Kyoto University Hospital, Kyoto, Japan.
[8]Center for iPS Cell Research and Application, Kyoto University, Kyoto, Japan.
*Current affiliation: Department of Orthopaedic Surgery, Nagahama City Hospital, Nagahama, Japan.
†Current affiliation: Department of Orthopaedic Surgery, Kobe City Medical Center General Hospital, Kobe, Japan.
‡Current affiliation: Innovative Clinical Research Center, Kanazawa University, Kanazawa, Japan.
§Current affiliation: Department of Orthopaedic Surgery, National Hospital Organization Kyoto Center, Kyoto, Japan.

cells gradually lose their mechanical properties and eventually collapse, causing articular surface deformities.[1–3]

Several staging and classification systems have been applied to diagnose ION, and the system proposed by the Specific Disease Investigation Committee (SDIC) has been used in Japan, which is a modified version of the system proposed by the Association Research Circulation Osseous (ARCO) Committee.[4] This staging system includes stage 1 (specific findings of osteonecrosis are observed on magnetic resonance imaging [MRI], bone scintigram, or histology, not on X-ray images), stage 2 (demarcating sclerosis is seen without collapse of the femoral head), stage 3 (collapse of the femoral head, including the crescent sign, is seen without joint-space narrowing. Mild osteophyte formation of the femoral head or acetabulum may be seen), and stage 4 (osteoarthritic changes are seen). Stage 3 was subdivided into stage 3A (collapse of the femoral head being less than 3 mm) and stage 3B (collapse of the femoral head being 3 mm or greater).[4] Although the natural history of ION depends on the etiological background of each case, this condition is considered to be a progressive disease from the early stage (stage 1), with minimum necrotic areas found only by MRI, to the advanced stage (stage 4), with painful osteoarthritis of the hip joint.[4,5] Regarding the surgical treatment of patients at early stages (stage 1 or 2), core decompression has been widely used to decompress elevated pressure in the femoral head.[5–7] Although this procedure may be effective for some patients, the results are unpredictable.[7] Total hip arthroplasty (THA) is the only way to treat patients at the terminal stage (stage 4).[1,3] The survival rate of THA has markedly improved owing to the advancement of materials and surgical technology.[3] However, THA should be avoided as much as possible, because patients with ION are relatively young, therefore, joint-preserving treatment for patients at stage 3 is a critical issue. Sugioka's rotational osteotomy, which replaces the weight-bearing area with intact bone tissues, has been used for stage 3 patients and was shown to be effective in some patients.[8] However, the application of this surgery is limited for patients with intact areas.[9] Because the loss of blood supply and bone-forming cells are causative for this condition, grafting vascularized bones is a theoretically reasonable way to treat this condition.[10] Clinical results appear to depend on the size of the necrotic area and the prolonged period required to generate new bone tissues,[10] possibly due to the decreased number of bone-forming cells.[11,12]

The application of concentrated bone marrow cells (BMCs) to ION was initiated by Hernigou.[13] He invented a method to transplant BMCs after core decompression and performed it on a large number of patients at early stages. The effect of transplantation was not clear because of the lack of controls in his studies.[14] Gangji *et al.* conducted prospective randomized studies and reported that the application of concentrated BMCs significantly delayed progression of the disease,[15,16] and its effect continued 5 years after transplantation.[16] The clinical results of this method depended at least partly on the number of osteogenic cells in aspirated BMCs, which could not be controlled.[11]

Multipotent mesenchymal stromal cells (MSCs) are promising materials for regenerating the musculoskeletal system.[17,18] MSCs are defined as plastic dish-adherent cells that can be differentiated to cells in osteogenic, chondrogenic, and adipogenic lineages *in vitro*.[19,20] MSCs may also be able to differentiate to vascular endothelial cells.[21] They are found in several different tissues,[17] among which bone marrow stroma is a representative home of MSCs; therefore, the therapeutic effect of BMCs for ION may depend on the effect of MSCs. The application of MSCs expanded *in vitro* for ION was considered to overcome the issue of the unstable number of BMC treatment, and Zhao conducted a prospective randomized trial using *in vitro*-expanded MSCs and reported that cultured MSC transplantation in combination with core decompression surgery was effective in delaying and avoiding femoral head collapse.[22] Although these findings suggest the promising role of MSCs on ION, this was also shown to be ineffective for patients at advanced stages such as stage 3.[22]

We previously designed a treatment with a combination of MSCs and vascularized bone grafts to apply MSCs for advanced stages, and performed a preclinical study using an animal model.[23] Based on the promising results of that study, we proceeded to clinical trials and herein we report the result.

Materials and Methods

Study design

This study was a prospective, open-labeled, proof-of-concept clinical trial conducted in the Kyoto University Hospital. Patient registration and data management were performed in the Department of Clinical Trial Design and Management, Translational Research Center, Kyoto University Hospital. This clinical study was registered to the UMIN Clinical Trials Registry (UMIN000001601). The study protocol was approved by the Ethics Committee of Kyoto University Graduate School and Faculty of Medicine, Guidelines on Clinical Research using Human Stem Cells of Ministry of Health, Labour and Welfare, Japan (www.mhlw.go.jp/bunya/kenkou/iryousaisei06/pdf/111201_ 1.pdf) and was conducted according to the Declaration of Helsinki. Results were evaluated 24 months after the treatment, and the primary endpoint was the progression of the radiographic stage and the secondary endpoint was bone volume changes evaluated by computed tomography (CT), and clinical score.

Patients eligibility

Eligibility criteria were between 20 and 50 years of age and the presence of necrotic stage 3A or 3B according to the radiographic stage system by the SDIC.[4] The radiographic stage was evaluated also by the Steinberg classification.[24]

Exclusion criteria were patients with a surgical history on the affected part, heavy smokers (Brinkman index > 600) requiring the continued use of warfarin, diabetes mellitus (defined by HbA1c > 9.0%), arteriosclerosis obliterans, pregnancy, malignant disease, myocardial infarction, brain infarction, rheumatoid arthritis, patients receiving dialysis, blood disease (leukemia, myeloproliferative disorder, and myelodysplastic disorder), patients with a limited life expectancy, hepatitis B, hepatitis C, human immunodeficiency virus and syphilis, hypotension (systemic volume < 90 mmHg), low body weight (< 40 kg), loss of marrow function (neutrophils < 1500/mm^3, hemoglobin < 11.0 g/dL [men], 10.0 g/dL [women], platelets < 100,000/mm^3), patients whose drugs (osteoporosis and steroids) were changed within 3 months

of the clinical study, and ineligible patients for the clinical study as decided by a doctor.

Assessment of necrotic lesions

The necrotic lesion and the size were assessed by the radiographic classification proposed by the Japanese Investigation Committee.[4] Type A lesions occupied the medial one-third or less of the weight-bearing portion. Type B lesions occupied the medial two-thirds or less of the weight-bearing portion. Type C1 and type C2 lesions both occupied more than the medial two-thirds of the weight-bearing portion, wherein type C2 lesions extended laterally to the acetabular edge, whereas type C1 lesions did not.[4]

Preparation of autologous bone marrow-derived MSC

Peripheral blood (400 mL) was obtained from patients and incubated at room temperature for 3 h to proceed coagulation. Serum was then separated by centrifugation at 1500 *g* for 15 min, collected, and stored at −30°C. This procedure was repeated once after 7 days; therefore, autologous serum from 800 mL was prepared from each patient.

The isolation of bone marrow-derived MSCs from patients was performed as described previously.[25] Briefly, bone marrow (100 mL) was aspirated under general anesthesia from two sites of each right and left posterior iliac crest using a bone marrow harvest needle (Angiotech, Gaineville, FL). Aspirated bone marrow (25 mL) was immediately mixed with 1000 IU heparin (Mochida Pharmaceutical Co., Tokyo, Japan) and transported to the cell processing center. Mononuclear cells containing MSCs were seeded at a density of 2.5×10^5 cells/cm^{2}and cultured with the α-minimal essential medium with GlutaMAX (Invitrogen Co., Carlsbad, CA) supplemented with 10% autoserum, 100 U/mL penicillin, and 100 mg/mL streptomycin, under 20% pO_2 and 5% pCO_2 conditions at 37°C. When the total cell number reached 5.0×10^7, cells were dissociated by TripLE Select (Invitrogen Co.), frozen with cryoprotectant (CP-1; Kyokuto Pharmaceutical Ind. Co., Tokyo, Japan), and stored in liquid nitrogen. Frozen cells were thawed and recultured at a density of 1.35×10^4 cells/cm^2 under the same condition for 4 days before transplantation surgery. The cells were dissociated by TripLE Select, washed by serum, and prepared in suspension 2 h before transplantation. The survival rate was calculated after thawing and at the timing of shipping.

Evaluation of multipotent MSCs

Differentiation potential. The potential for differentiation in osteogenic, adipogenic, and chondrogenic directions was examined as previously reported using the differentiation induction protocol provided by Cambrex (East Rutherford, NJ) in each MSC of the sampled cells from the preceding MSC. Osteogenic differentiation was evaluated by Alizarin Red S staining on day 14 of induction. Adipogenic differentiation was evaluated by Oil Red O staining on day 21 of differentiation, in which cells were stained with 40 mM pH 4.2 Alizarin Red S (Sigma-Aldrich, St. Louis, MO). After 21 days of adipogenic differentiation, cells were stained with 0.3% Oil Red O (NacalaiTesque, Kyoto, Japan). After 21 days of chondrogenic differentiation, pellets were stained with Alcian Blue (Muto Pure Chemicals Co., Ltd., Tokyo).

Cytogenetic analysis. G-band cytogenetic analysis was performed on isolated mononuclear cells and a sample of final transplanted MSCs. A minimum of 20 metaphases were analyzed in each case. The criteria used to describe a cytogenetic clone and description of the karyotype followed the recommendations of the International System for Human Cytogenetic Nomenclature.[26]

Measurement of endotoxin. The activity of endotoxin in the supernatant of final transplanted MSCs was assayed by the limulus test using the limulus ES-II single test kit (Wako, Osaka, Japan).

In vivo tumor formation assays. Nonobese diabetic (NOD)-severe combined immunodeficient (SCID) mice were purchased from Shimizu Laboratory Supplies (Kyoto, Japan). *In vivo* experiments were approved by the Institutional Animal Research Committee, and were performed according to the Guidelines for Animal Experiments of Kyoto University. A fraction of final transplanted MSCs (5.0×10^6) was sampled and inoculated subcutaneously into the right flank of each mouse. Tumor formation was monitored for 6 months, and mice were then euthanized and the existence of tumors was assessed.

Transplantation surgery

Patients were placed in a supine position on the table. A curved skin incision (modified Smith-Peterson approach) was prepared from the iliac crest to the anterior aspect of the proximal thigh. The anterior aspect of the femoral neck was explored and a cortical window (1.5 × 4 cm) was made, through which a bony trough connecting to the necrotic area was formed under X-ray fluoroscopy.[27,28] Necrotic areas, including sclerotic bones, were extensively curetted under the fluoroscopy and endoscopy. MSCs ($0.5–1.5 \times 10^8$) premixed with β-tricalcium phosphate (β-TCP) granules (Osferion; Olympus Terumo Biomaterials Co., Tokyo, Japan) were transplanted into the cavity. The tricortical iliac bone (1.5 × 2 × 5 cm) with a vascular pedicle (deep circumflex iliac vessels) was then harvested and grafted into the bone trough.[27,28]

Postoperative course

Patients were kept non-weight bearing for 6 weeks, followed by partial bearing for the next 6 weeks. The return to sports and work was allowed for the next 6 months confirming ossification. Clinical and radiological evaluations were performed according to the protocol until 24 months after surgery.

Evaluation of treatment

The primary endpoint in this study was radiographic progression of osteonecrosis by anteroposterior radiographs at the point of pretreatment and 2 years after treatment. Progression was evaluated according to the radiographic clinical stage established by the SDIC with modifications to the latest version of the ARCO staging system[4] and Steinberg classification.[24]

Bone volume was calculated from CT images. CT images consisted of 400 slices with a voxel size of 68.224 μm in all three axes. Coronal and sagittal cross-sectional views of the

femoral head were reconstructed using adjunctive software. Image reconstruction and quantification of the femoral head were performed with VG Studio MAX software (Nihon Visual Science, Tokyo, Japan). The femoral head was defined as an upper lesion on the line between the epiphysis edge of the inside and outside. The bone volume of the femoral head was calculated by VG Studio MAX software. These radiographic results were evaluated by three outside reviewers (two orthopedic surgeons and one radiologist) who were unrelated to this clinical trial.

Clinical symptoms were evaluated by the hip score defined by the Japanese Orthopaedic Association (JOA).[29]

Adverse events

In this clinical trial, adverse events were defined as any event occurred during the entire study period regardless of the relationship with the protocol, and monitored in the Department of Clinical Trial Design and Management, Translational Research Center. Serious adverse events were assessed by the External Data Monitoring Committee.

Statistical analysis

Continuous variables are described as the mean and standard deviation. Radiographic progression of osteonecrosis was assessed by the Wilcoxon's signed-rank test. Changes in bone volume and the clinical score according to the JOA score were examined by the paired *t*-test. All reported p-values were two sided, with a value below 0.05 being considered significant. All statistical analyses were conducted in the Department of Clinical Trial Design and Management, Translational Research Center using SAS version 9.2 (SAS Institute, Cary, NC).

Results

Baseline data of patients

Between November 2007 and June 2009, 10 patients were recruited into the clinical trial. All patients were male and the average age was 31.7 (range 20–48) years, and previous history of steroid treatment was found in four patients (Table 1). The pretreatment radiographic stage was stage 3A on six hips and stage 3B on four hips according to the SDIC System, and stage 3 on six hips and stage 4 on four hips by the Steinberg classification (Table 2). Pretreatment bone volumes averaged 56.5 (range 45.3–66.4) cm^3. Pretreatment clinical scores according to the JOA averaged 65.6 (range 33–95) points (Table 2).

Cell characteristics of manufactured MSCs

The preparation of autoserum and harvesting, culturing, and storing of MSCs were safely conducted in all cases. The number of isolated mononuclear cells from bone marrow varied among cases ($0.95–2.31 \times 10^7$/mL), with the expected number of cells (5.0×10^7) being obtained within 10 days in all cases, except for case 9, in which 16 days were required (Table 1). The mean survival rate of frozen MSCs after thawing was 93.6% (89.2–97.3%) (Table 1). The mean population doubling and doubling time after thawing was 1.07 (0.41–1.68) and 106.4 h (57.2–232.1 h), respectively, and the mean survival rate of shipping cells was 97.1%

TABLE 1. CHARACTERISTICS OF PATIENTS AND TRANSPLANTED CELLS

Case	*Age/ gender*	*Past illness*	*History of steroid*	*Concentration of isolated MNCs from bone marrow* ($\times 10^7$/mL)	*Total number of seeded MNCs* ($\times 10^9$)	*Culture period (day)*	*Total number of stored MSCs* ($\times 10^7$)	*Fraction of living cells after thawing (%)*	*Population doubling after thawing*	*Population doubling time (hr)*	*Fraction of living cells at shipping (%)*	*Chromosomal aberration*
1	27/M	Nephritis	Yes	1.54	1.00	9	6.38	89.5	0.41	232.1	97.3	No
2	23/M	Cushing syndrome	Yes	1.47	1.00	9	14.38	87.7	0.61	156.5	91.8	No
3	48/M	Meningioma	No	2.25	1.37	9	9.88	93	0.92	104.5	98.0	No
4	20/M	Hepatitis	Yes	2.28	1.14	8	11.94	92.6	1.15	83.5	92.0	No
5	35M	NP	No	1.08	0.65	9	7.00	96.5	1.30	73.9	12.3	No
6	28/M	NP	No	2.06	1.29	10	6.75	97.1	1.68	57.2	96.0	No
7	39/M	Leukemia	Yes	2.31	1.31	9	14.00	95.5	0.82	117.7	98.0	Yes[a]
8	26/M	NP	No	2.18	1.13	9	16.13	97.3	1.00	96.0	100.0	No
9	33/M	NP	No	0.95	0.90	16	6.56	97.2	1.15	83.5	96.0	No
10	38/M	NP	No	1.77	0.98	8	16.56	89.2	1.63	59.0	97.0	No

[a]46,XY,add(1)(q11),−2,−4, add(7)(q11.1),−22, +3mar.
MSCs, mesenchymal stromal cells; MNC, mono nuclear cell; NP, nothing particular.

TABLE 2. RADIOLOGICAL AND CLINICAL RESULTS

		Stage							
		ARCO[b]		Steinberg		Bone volume (cm^3)[c]		Clinical score (JOA)	
Case	Class[a]	Before Tx	2 year after Tx	Before Tx	2 year after Tx	Before Tx	2 year after Tx	Before Tx	2 year after Tx
1	C2	3B	3B	3	4	45.3	46.8	33	93
2	C2	3A	3A	3	3	65.4	68.8	96	100
3	C2	3B	4	4	5	43.6	38.3	36	39
4	C1	3A	3A	4	4	66.4	69.7	95	100
5	C2	3A	3A	3	3	58.3	60.2	79	95
6	C2	3A	3A	3	4	60.4	60.6	52	95
7	C2	3B	4	4	6	57.1	51.0	84	84
8	C2	3B	3B	4	4	56.0	58.0	56	90
9	C2	3A	3A	3	3	64.8	65.9	88	95
10	C2	3A	NA	3	NA	47.4	NA	37	NA

[a]Radiographic clinical classification proposed by Japanese Investigation Committee.
[b]Latest modification of ARCO staging score by Japanese Investigation Committee.
[c]Bone volume of femoral head calculated from computed tomography.
ARCO, Association Research Circulation Osseous; JOA, Japanese Orthopaedic Association; NA, not analyzed; Tx, treatment.

(92.0–100%) (Table 1). The differentiation properties to the osteogenic, adipogenic, and chondrogenic lineages were confirmed in MSCs (data not shown). No tumorous condition was found in any SCID mice during the 6 months following inoculation. A chromosomal aberration (46,XY, add(1)(q11), −2,−4, add(7)(q11.1), −22, +3mar was detected in one case (case 7, Table 1). An identical aberration was found in BMCs immediately after they were isolated, suggesting that this aberration may not have been related to the *in vitro* culture process. Endotoxin activity was not detected in the supernatant of MSCs.

Transplantation

During surgery, as much of the necrotic area was removed as possible. The average bone defect was 9.3 cm^3 (2.0–20.0 cm^3). The average number of transplanted MSCs was 1.2×10^8 ($0.5–1.5\times10^8$) and the average volume of β-TCP granules was 3.3 g (1.5–5.0 g).

Radiographic progression of the stages

One patient who had bilateral lesions and decided to receive surgery for contralateral hip joints was excluded from this study, 12 months after the treatment. The other nine patients completed the planned follow-up course and were eligible for the evaluation. None of the stage 3A patients progressed to stage 3B or 4 (Figs. 1A and 2). Two hips of stage 3B (50%) did not progress (Fig. 1A), while the remaining two hips (50%) progressed to stage 4 twelve months after the treatment (Fig. 1A).

According to the Steinberg classification, two of six hips (33%) with stage 3 progressed to stage 4. One of four hips (25%) with stage 4 progressed to stage 5 and one hip (25%) progressed to stage 6. The remaining two hips (50%) maintained the shape of the femoral head. The etiology of the progressed hips was idiopathic in one hip and steroid induced in one hip, and past illnesses of these cases were meningioma in one hip and leukemia in one hip. Patient ages were 48 and 38 years. The radiographic clinical classification was type C2 in both cases.

Changes in the bone volume

Bone volume of the femoral head according to CT was evaluated before treatment, 1 year after treatment, and 2 years after treatment. Average bone volume before treatment was $56.5\pm8.4cm^3$ (Fig. 1B). Average bone volume significantly increased to $57.9\pm9.0\,cm^3$ 1 year after treatment ($p=0.005$, Fig. 1B). Average bone volume maintained at $57.7\pm10.6\,cm^3$ 2 years after treatment (Fig. 1B). However, bone volume decreased in progressed cases (43.6–38.3 cm^3 and 57.1–50.9 cm^3, Table 2).

Clinical score

The clinical score according to the JOA was evaluated before treatment, 1 year after treatment, and 2 years after treatment. The average JOA score before treatment was 65.6 ± 25.5 points (Fig. 1C). The JOA score significantly improved to 90.2 ± 14.1 points with statistic difference at 1 year after treatment (Fig. 1C). The JOA score maintained at 87.9 ± 19.0 points 2 years after treatment ($p=0.028$, Fig. 1C). The JOA score did not markedly improved in progressed cases (36–39 and 84–84, Table 2).

Adverse events

Sixty-one adverse events were observed in ten patients (Table 3). One serious adverse event was a case of medial meniscus tear in the contralateral knee joint. An external evaluation judged that this serious adverse event was not correlated to the current clinical study. Remaining sixty adverse events were nonserious adverse events. The frequently reported adverse events were an increase in creatine phosphokinase, increase in C-reactive protein, anemia, pain in the hip joint, decrease in albumin, complications at the wounded area, decrease in total protein, wound pain, and fever (Table 3). In one case, the vascular pedicle of the transplanted bone

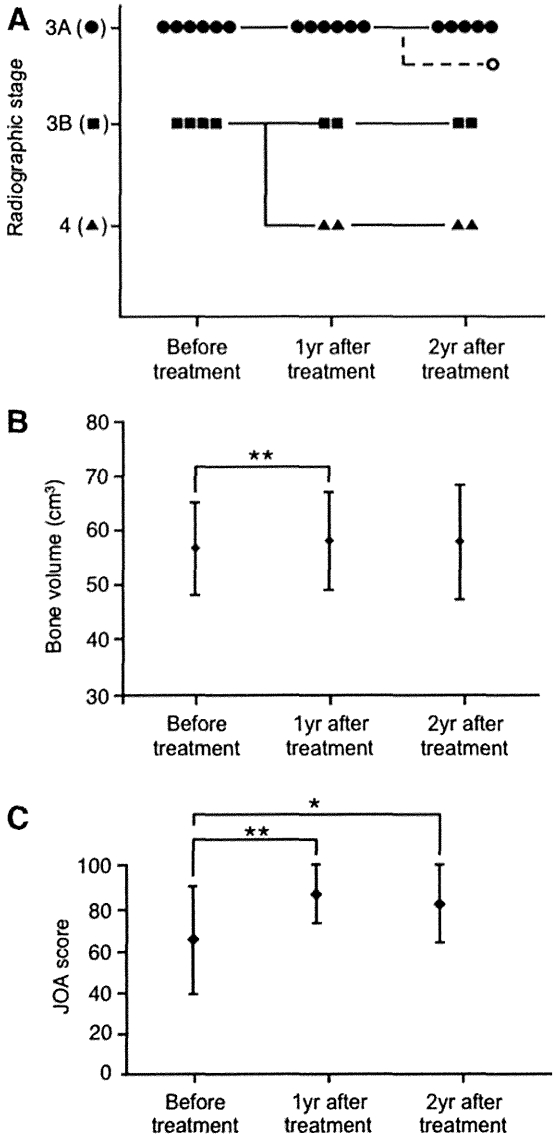

FIG. 1. Radiological and clinical results of treatment. **(A)** Transition of the radiographic stage. The radiographic stage of each case at the indicated time points was evaluated by the system of Specific Disease Investigation Committee (SDIC), which is a modified version of the system proposed by the Association Research Circulation Osseous (ARCO) Committee.[4] One case of stage 3A before treatment was off-protocol after 1 year. **(B)** Bone volume in the femoral head. Bone volume in each femoral head was calculated from data on computed tomography (CT) scans at each time point. $^{**}p<0.01$. **(C)** Clinical results. Clinical results were evaluated by the Japanese Orthopaedic Association (JOA) hip-score[29] at each time point. $^{**}p<0.01$, $^{*}p<0.05$.

was injured during surgery, and the injured part of the vessels was microsurgically replaced by vein grafts and its patency was confirmed by a CT angiogram.

Discussion

The prognosis of ION is influenced by the size of the necrotic area, stage of the disease, time from the diagnosis, and etiological factors.[4,9,30] According to the radiographic classification proposed by the SDIC, types A and B are less likely to progress to collapse than types C1 and C2.[4,30] These results suggest that broad necrotic lesions on weight-bearing areas increase the risk of disease progression. The stage of disease is also an important factor that may influence the treatment.[4,30] Core decompression surgery is commonly used in precollapse stages such as stage 2. Based on the clinical results reported by Hernigou, Gangji, and Zhao, the combination of core decompression with *in vitro* expanded MSCs was shown to be an appropriate approach for stage 2 with lesions defined as class A or B.[12,14,22] Application of the biomaterial as a scaffold of MSCs reported by Nöth *et al.* may be an alternative choice for the treatment of patients with this condition.[31]

Core decompression surgery was performed less than vascularized bone graft surgery in the mild collapse stage corresponding to a subchondral fracture (stage 3).[32,33] Vascularized bone graft surgery has the benefits of supplying living cells and mechanical strength. Kawate *et al.* published a case report on cell therapy combined with vascularized fibular grafts for ION.[34] They cultured autologous MSCs with β-TCP granules *in vitro*, induced osteogenic differentiation and transplanted the necrotic area with a vascularized fibular graft.[34] In the present study, we used undifferentiated MSCs instead of differentiated osteogenic cells, which was based on the findings of our previous preclinical study.[23] A comparative study should be performed to investigate which type of cell therapy is suitable for the treatment of ION.

The safety and efficacy are critical points in any cell therapy, and the major purpose of our study is also to evaluate these points. As for the safety, we evaluated the characteristics of cultured cells and adverse effects on patients during the entire course of therapy. No serious events were observed in any case during establishing and expanding cells such as bacterial contamination. One serious risk of cell transplantation is the transformation during *in vitro* expansion.[35] Previous studies have described the spontaneous transformation of MSCs during *in vitro* processing,[36,37] which was shown to be caused by contaminated cancer cells.[38–40] This may happen in laboratories in which cancer cells were cultured in the same area. Cells for clinical use should be prepared in an area defined by Good Manufacturing Practice, in which the culture of other cells, particularly established cancer cells, should be strictly forbidden.[41] Cell transplantation in immunodeficient mice is one of standard methods used to evaluate transformation,[35] and we did not observe tumorous conditions in NOD-SCID mice transplanted with MSCs in this series. Chromosome analysis is another method that can predict transformation. Physiological stress during *in vitro* culture has been suggested to induce chromosomal aberrations, which may be the case even if the cell processing system is of a clinical grade.[42] In the present study, chromosomal aberrations were not found in transplanted MSCs, except for one case (case 7). This patient received intensive chemotherapy for leukemia 13 years ago and was free from the disease at the entry for the current study. The aberration was also detected in BMCs before expansion, excluding the effect of culture process. Cultured MSCs in this case showed no definite abnormalities during *in vitro* expansion or in their differentiation properties. A careful long-term follow-up should be undertaken in this case.

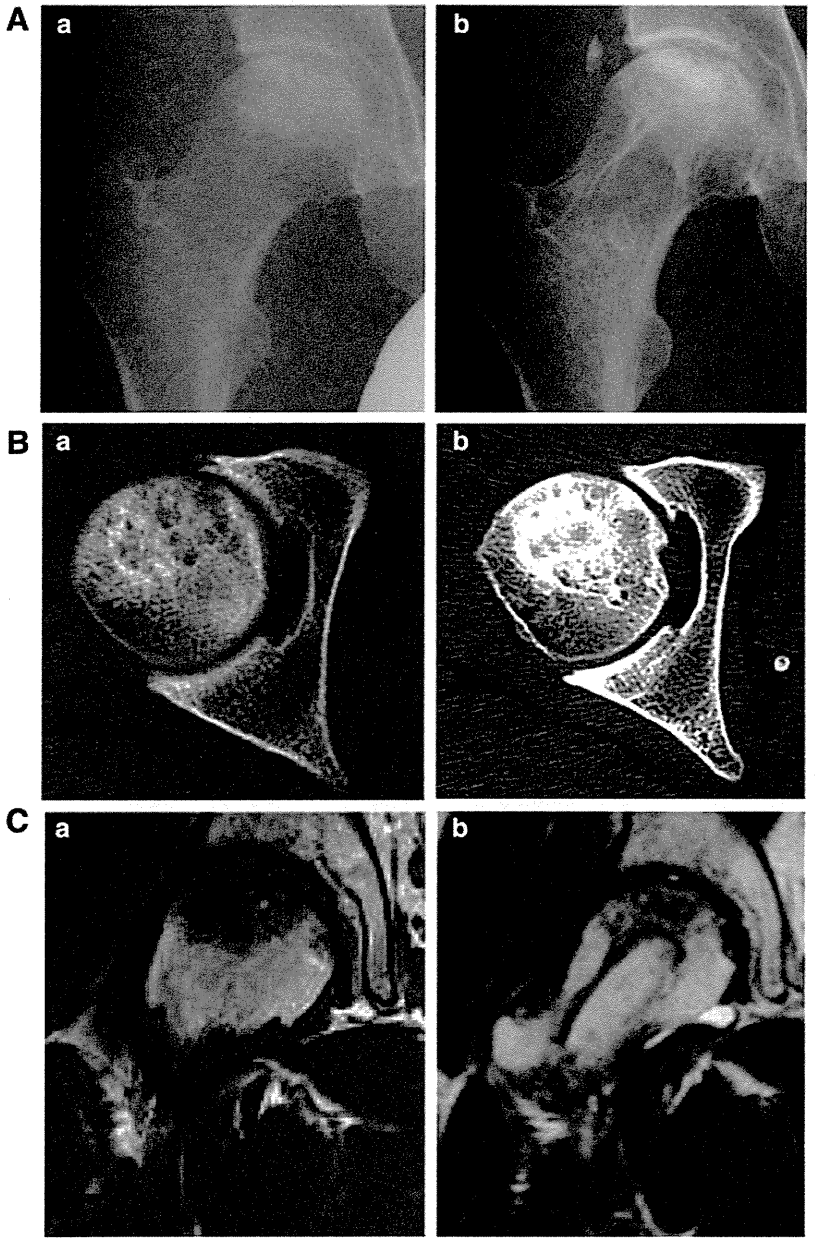

FIG. 2. Case presentation. A 33-year-old man (case 9) with idiopathic osteonecrosis of the femoral head. **(A)** Anteroposterior radiographs of the femoral head before **(a)** and 2 years after surgery **(b)**. The radiographic stage and classification before treatment were 3A and type C2, respectively (b). **(B)** Transverse CT image of the femoral head before **(a)** and 2 years after treatment **(b)**. **(C)** Frontal view of the femoral head by T1-weighted magnetic resonance imaging before **(a)** and 2 years after treatment **(b)**.

During the entire course, one serious and sixty adverse events were observed (Table 3). There were two adverse events correlated with cell preparation. One was vertigo (1/10) after blood sampling for preparation of autoserum, and the anemia (9/10) for preparation of autoserum and bone marrow aspiration. One serious adverse event (knee meniscus tear) was evaluated not to be related to the clinical study. Although it is difficult to completely deny the effect of transplanted MSCs, almost all other adverse events were those found in surgical procedures without cell transplantation. For example, the increase of creatine phosphokinase was almost always observed after the surgery involving muscles, and in the current surgery, muscles attaching iliac bone were severed for harvesting bone grafts. The increase of C-reactive protein, anemia, and decrease in albumin and total protein were also observed in major orthopedic surgeries. Without saying, even if the effect of adverse events is minimum, it is rational to consider these adverse events based on the risk–benefit balance. For example, we used general anesthesia for harvesting bone marrow, which potentially has a considerable risk. When the efficacy of the current method is precisely evaluated, the risk associated with each procedure should be reconsidered.

Because of the small sample number and lack of control, only limited information was obtained for efficacy in this study. Two of nine cases in this study showed the progression of stages evaluated by the SDIC system. In both cases, we observed the formation of cystic lesions in the femoral head 12 months after surgery. β-TCP degradation began from two to 3 weeks *in vivo*.[43,44] An imbalance between bone resorption and formation may cause such a condition, and further study is required to define the suitable amount of β-TCP to be used in cell transplantation therapy. We compared the current results with those of simple vascularized iliac bone grafting performed during